

3D NUMERICAL SOLUTION OF AERO-NOISE WITH HIGH-ORDER DISCONTINUOUS GALERKIN METHOD

Lü Hongqiang (吕宏强), Sun Qiang (孙强), Qin Wanglong (秦望龙)

(College of Aerospace Engineering, Nanjing University of Aeronautics
and Astronautics, Nanjing, 210016, P. R. China)

Abstract: The flow-induced noise is simulated with a hybrid method. Firstly, a steady-state background flow field is given by solving Reynolds averaged Navier-Stokes(RANS) equations with finite volume (FV) method on structured grid. Then the linearized Euler equations(LEE) can be constructed based on the resulted background flow field, where the source term on the right hand side is computed using stochastic noise generation and radiation (SNGR) method. Finally, the unsteady acoustic field is obtained through solving LEE using high-order discontinuous Galerkin(DG) method on unstructured grid, where the parallel computing based on mesh partitioning and a "Quadrature-Free Implementation" method for high-order DG are employed to accelerate the computation. In order to demonstrate the sound propagation in detail, a visualization method for high-order schemes is also developed here. Moreover, in order to test the validation and the accuracy, a 3D cavity test in comparison with the experimental data is displayed first in this paper, then a 3D high-lift wing is also simulated to demonstrate its capability for very complex geometries.

Key words: aero-noise; discontinuous Galerkin; linearized Euler equations; complex geometry; stochastic noise generation and radiation

CLC number: V211.3

Document code: A

Article ID:1005-1120(2013)03-0227-05

INTRODUCTION

In recent years, the flow-induced aero-noise problems have been becoming more and more attractive. However, it is still a challenging problem for numerical simulation since it has multi-scale properties^[1]. In theory, the direct numerical simulation(DNS) and the large eddy simulation(LES)^[2] should be promising for aero-noise problems. However, they are still far away from solving 3D complex geometries due to their computational cost. Hybrid approaches coupling the computational fluid dynamics (CFD) and the computational aeroacoustic (CAA) are widely used for 3D engineering problems, where highly accurate numerical schemes are still needed for capturing the broadband property.

High-order finite difference (FD) meth-

ods^[1,3] which are widely used for DNS and LES are also employed for acoustic computation, where high-quality structured mesh is normally required. An alternative is the high-order discontinuous Galerkin (DG) method^[4-12] which is well suited to unstructured grid. However, the numerical cost of high-order DG methods is expensive since there are more degrees of freedom on each element. Atkins and Shu introduced the "Quadrature-Free Implementation"^[9] to transfer the numerical integration which dominates the numerical expense to matrix-vector multiplication, which can dramatically reduce the CPU time in high-order cases. Another widely-used way to accelerate the computation is parallel computing since only the information on the elements neighboring partition boundary is needed to be ex-

Foundation items: Supported by the Aeronautical Science Foundation of China (20101552018); the National Natural Science Foundation of China (11272152).

Received date: 2012-12-08; **revision received date:** 2013-01-15

Corresponding author: Lü Hongqiang, Associate Professor, E-mail: hongqing.lu@nuaa.edu.cn.

changed between partitions. High-order DG methods have been used for some benchmark sound propagation problems and low-order DG has also been employed for simple geometries such as cavity^[13].

In this paper, a parallel high-order DG is used to solve LEE which is resulted from a pre-computed steady-state background flow-field. The stochastic noise generation and radiation (SNGR) method is used to construct the source term of LEE. Parallel computing and "Quadrature-Free Implementation" are both employed to make the computation more efficient and a visualization method is developed to demonstrate the acoustic information. Numerical results indicate that the broad-band property of the turbulence-induced noise can be captured even on very coarse grid and the method is well-suited for very complex geometries.

1 COMPUTATION SCHEME

1.1 Governing equation

LEE in conservation form is given by

$$\frac{\partial \mathbf{U}'}{\partial t} + \nabla \cdot \mathbf{F}(\mathbf{U}', \mathbf{U}^0) = \mathbf{S} \quad (1)$$

where $\mathbf{U}' = (\rho', u', v', w', p')$ are the perturbation variables, $\mathbf{U}^0 = (\rho^0, u^0, v^0, w^0, p^0)$ the background flow-field variables and \mathbf{S} is the source term constructed with the SNGR method developed by Bailly^[14] based on the given steady-state background flow-field.

1.2 DG discretization

After applying the high-order DG discretization the following system is obtained

$$\int_e \phi'_i \frac{\partial \mathbf{U}'}{\partial t} d\Omega - \int_e \nabla \phi'_i \cdot \mathbf{F}(\mathbf{U}', \mathbf{U}^0) d\Omega + \int_{\partial e} \phi'_i \mathbf{F}(\mathbf{U}', \mathbf{U}^0) \cdot \mathbf{n} d\Gamma = \int_e \phi'_i \mathbf{S} d\Omega \quad (2)$$

where e is the grid element, ∂e are element interfaces, ϕ' is the test function, and \mathbf{U} is written in high-order form

$$\mathbf{U}' = \sum_{j=1}^{N'} \mathbf{u}'_j \phi'_j \quad (3)$$

In order to perform "Quadrature-Free Implementation"^[8], \mathbf{U}^0 and \mathbf{S} also need to be represented in high-order form in Eq. (2), shown as

$$\mathbf{U}^0 = \sum_{j=1}^{N^0} \mathbf{u}^0_j \phi_j^0 \quad (4)$$

$$\mathbf{S} = \sum_{j=1}^N \mathbf{s}_j \phi_j \quad (5)$$

For the convenience of performing the "Quadrature-Free Implementation", the LLF numerical flux is employed here. For the integral on the element interface in Eq. (2), $\mathbf{F}(\mathbf{U}', \mathbf{U}^0) \cdot \mathbf{n}$ is replaced by

$$\mathbf{H}(\mathbf{U}'^{,e}, \mathbf{U}'^{,f}, \mathbf{n}) = \frac{1}{2} [\mathbf{F}(\mathbf{U}'^{,e}) \cdot \mathbf{n} + \mathbf{F}(\mathbf{U}'^{,f}) \cdot \mathbf{n} - \alpha(\mathbf{U}'^{,f} - \mathbf{U}'^{,e})] \quad (6)$$

The integrals in Eq. (2) can be computed using numerical integration methods, which dominates the entire computational cost. Here the "Quadrature-Free Implementation" method is employed, where the numerical integration can be transformed to matrix-vector multiplication.

1.3 Quadrature-free implementation

The integrals in Eq. (2) are usually evaluated using numerical integration methods, which dominates the entire numerical cost. Here a quadrature-free implementation method is employed, where the treatment for the integrals over elements is the same as the one developed by Atkins and Shu^[8], but the treatment for the integrals over element boundaries is slightly different.

As stated in Ref. [8], instead of evaluating the integral $\int_e \nabla \phi'_i \cdot \mathbf{F}(\mathbf{U}', \mathbf{U}^0) d\Omega$ using numerical integration, \mathbf{F} needs to be written in high-order form

$$\mathbf{F} = \sum_{j=1}^N \mathbf{f}_j \phi_j \quad (7)$$

where $\mathbf{f}_j = (f_{x,j}, f_{y,j}, f_{z,j})$ can be calculated using \mathbf{U}^0 and \mathbf{U}' . Then $\int_e \nabla \phi'_i \cdot \mathbf{F}(\mathbf{U}', \mathbf{U}^0) d\Omega$ becomes

$$\sum_{j=1}^N f_{x,j} \int_e \frac{\partial \phi'_i}{\partial x} \phi_j d\Omega + \sum_{j=1}^N f_{y,j} \int_e \frac{\partial \phi'_i}{\partial y} \phi_j d\Omega + \sum_{j=1}^N f_{z,j} \int_e \frac{\partial \phi'_i}{\partial z} \phi_j d\Omega \quad (8)$$

where the integral such as $\int_e \frac{\partial \phi'_i}{\partial x} \phi_j d\Omega$ can be evaluated only once.

Similarly, for the integrals over element boundaries, only the integrals such as $\int_{\partial e} \phi_i \phi_j d\Gamma$

need to be pre-computed using numerical integration method. Note that here ϕ_i and ϕ_j on ∂e are computed on the reference element and the mapping procedure in Ref. [8] can be skipped.

1.4 Time stepping

After the spatial high-order DG discretization, the full system can be written as

$$\frac{d\mathbf{U}'}{dt} = \mathbf{R} \quad (9)$$

where the 4-step Runge-Kutta time stepping is used to obtain the unsteady noise field

$$\begin{aligned} \mathbf{U}'_{n,0} &= \mathbf{U}'_n \\ \mathbf{U}'_{n,k} &= \mathbf{U}'_n + \gamma_k \Delta t \mathbf{R}_{n,k-1} \quad k=1, \dots, N \\ \mathbf{U}'_{n+1} &= \mathbf{U}'_{n,N} \end{aligned} \quad (10)$$

2 PARALLEL COMPUTING

It can be clearly observed from Eqs. (2, 5) that the variables in each element are only related to the variables in the neighboring elements, which makes DG methods very suited for parallel computing since the data exchange between partitions can remain local. Fig. 1 indicates that only the variables in the elements neighboring the partitioning boundary need to be transferred to the neighboring partition.

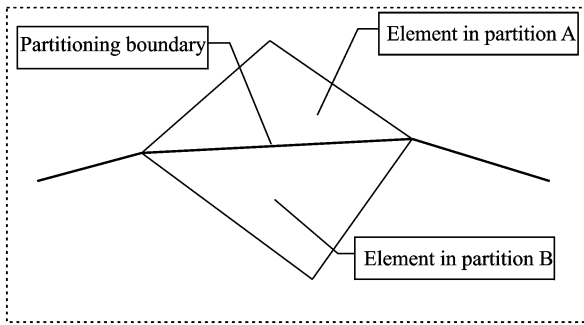
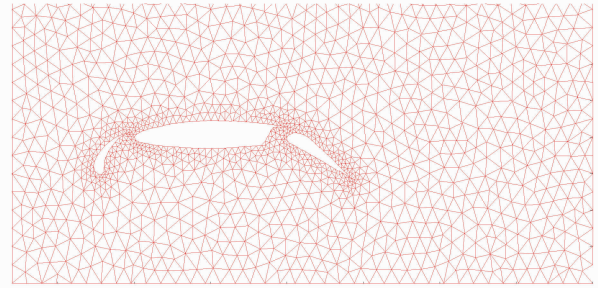


Fig. 1 Local data exchange for parallel computing

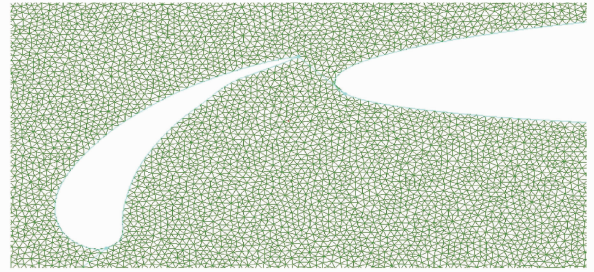
3 VISUALIZATION

If the obtained noise information is in high-order form (Eq. (3)), the widely used visualization tools, such as Techplot and Ensign, can not be used directly. Here a visualization mesh is generated independently, which is usually much finer than the computing mesh (Fig. 2). Then the value of \mathbf{U}' on each grid point of the visualization

mesh can be calculated with \mathbf{U}' on the computing mesh (Fig. 2). Finally, \mathbf{U}' on the visualization mesh can be visualized using Techplot and Ensign as usual, shown as Fig. 3.



(a) Computing mesh



(b) Visualization mesh

Fig. 2 Comparison of computing mesh and visualization mesh (2D case)

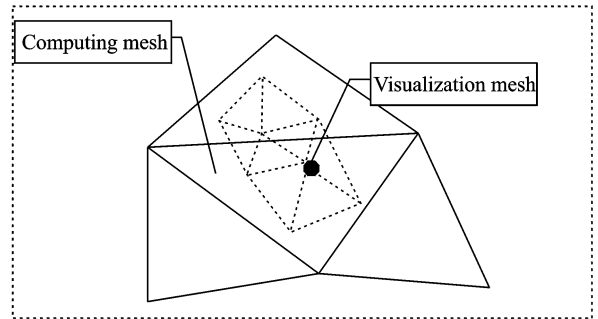


Fig. 3 Computation of \mathbf{U}' on visualization mesh

4 NUMERICAL RESULTS

4.1 Cavity

The flow-induced noise around a 3D cavity is first simulated using the introduced hybrid method. The steady-state background flow-field (Mach number $Ma=0.9$) is computed using FV on structured grid. The unsteady acoustic field is obtained using high-order DG ($p=3$) on relatively coarse unstructured grid which has only about 5 000 elements (Fig. 4). Fig. 5 displays the dis-

tribution of the perturbation pressure. The acoustic pressure spectrum matches well with the experimental result in Fig. 6 where the line is the numerical result and the points are the measurement results.

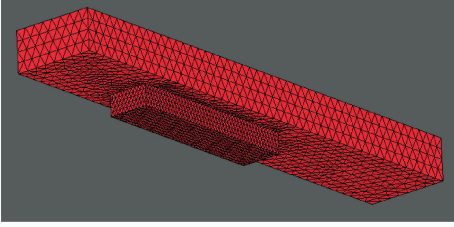
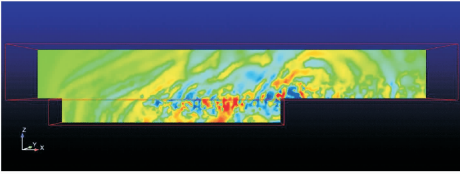
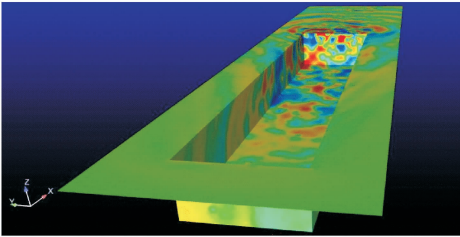


Fig. 4 Unstructured grid for noise simulation



(a) Distribution of perturbation pressure p' on symmetric profile



(b) Distribution of perturbation pressure p' on solid wall

Fig. 5 Distribution of perturbation pressure p'

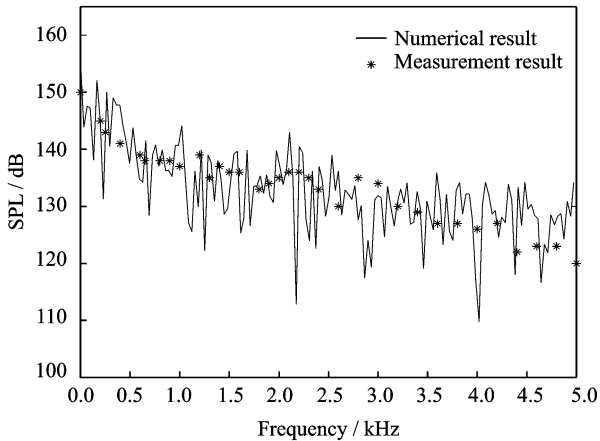


Fig. 6 Comparison of acoustic pressure spectrum

4.2 High-lift wing

The noise caused by a much more complex geometry, a high-lift wing (Fig. 7), is also computed here. The far-field inflow Mach number is

0.2 with the attack angle 10° . Fig. 8 displays the distribution of the perturbation pressure on $Z = 0.1, 0.5, 3.0, 4.0$ profiles and the solid surface of the wing, which indicates that the gaps between the flaps and the ailerons are the main source region of the aero-noise.

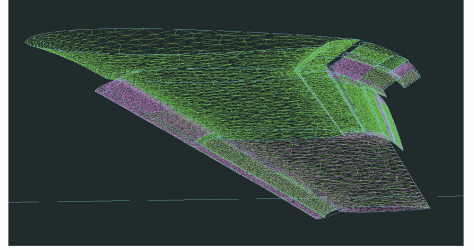
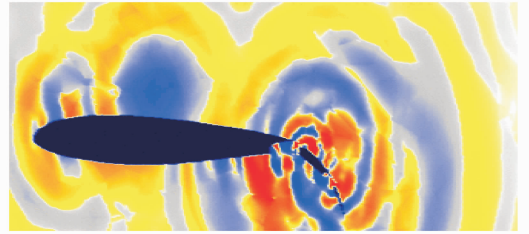
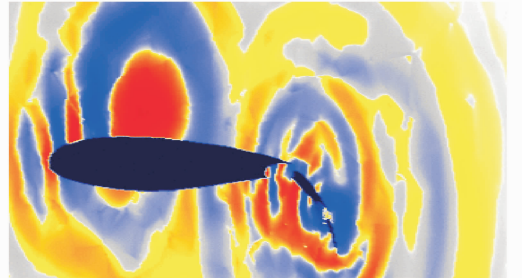


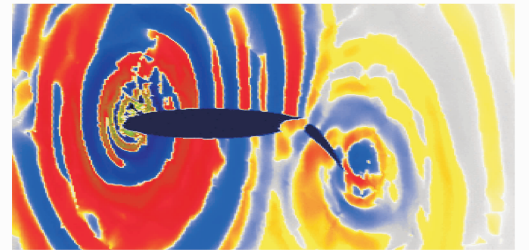
Fig. 7 High-lift wing



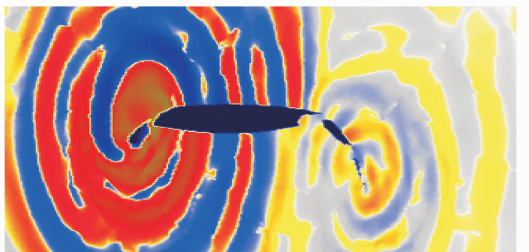
(a) Distribution of perturbation pressure p' on $Z=0.1$ profile



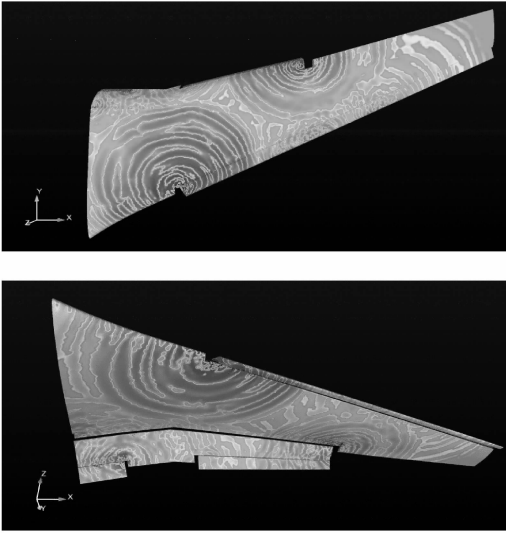
(b) Distribution of perturbation pressure p' on $Z=0.5$ profile



(c) Distribution of perturbation pressure p' on $Z=3.0$ profile



(d) Distribution of perturbation pressure p' on $Z=4.0$ profile



(e) Distribution of perturbation pressure p' on solid wall

Fig. 8 Distribution of perturbation pressure p'

5 CONCLUSIONS

(1) A hybrid method coupling CFD and CAA is employed to simulate the flow-induced aero-noise. The FV method is used to provide a steady-state background flow-field by solving RANS and the high-order DG is used to compute the unsteady acoustic field through solving the linearized Euler equations.

(2) The numerical method is quantitatively validated by testing the well-known cavity case. The numerical result matches well with the experimental data even when the acoustic computational grid is very coarse.

(3) The application of the numerical method to the high-lift wing indicates that this method is well suited for very complex geometries.

References:

- [1] Zhang Shuhai, Zhang Hanxin, Shu Chi-Wang. Topological structure of shock induced vortex breakdown[J]. *Journal of Fluid Mechanics*, 2009, 639: 343-372.
- [2] Wu Jingfeng, Ning Fangfei. Development of hybrid RANS/LES code and its validation[J]. *Transactions of Nanjing University of Aeronautics and Astronautics*, 2013, 30(1):24-32.
- [3] Deng Xiaogang, Zhang Hanxin. Developing high-order weighted compact nonlinear schemes[J]. *Journal of Computational Physics*, 2000, 165(1): 22-44.
- [4] Cockburn B, Kamiadakis G E, Shu Chi-Wang. *Discontinuous Galerkin methods: Theory, computation and applications*[M]. Berlin: Springer, 1999.
- [5] Bassi F, Rebay S. High-order accurate discontinuous finite element solution of the 2D Euler equations[J]. *Journal of Computational Physics*, 1997, 138(2): 251-285.
- [6] Lu Hongqiang, Wu Yizhao, Zhou Chunhua, et al. High resolution of subsonic flows on coarse grids[J]. *Acta Aeronautics et Astronautics Sinica*, 2009, 30(2): 200-204. (in Chinese)
- [7] Lu H Q. *High-order finite element solution of elastohydrodynamic lubrication problems*[D]. UK: University of Leeds, 2006.
- [8] Lu Hongqiang, Zhu Guoxiang, Song Jiangyong, et al. High-order discontinuous Galerkin solution of linearized Euler equations[J]. *Chinese Journal of Theoretical and Applied Mechanics*, 2011, 43(3): 621-624. (in Chinese)
- [9] Atkins H L, Shu Chi-Wang. Quadrature-free implementation of discontinuous Galerkin method for hyperbolic equations[J]. *AIAA Journal*, 1996, 36(5): 775-782.
- [10] Zhang L P, Liu W, He L X, et al. A class of hybrid DG/FV methods for conservation laws I: Basic formulation and one-dimensional systems[J]. *Journal of Computational Physics*, 2012, 231(4):1081-1103.
- [11] Liu Meilin, Liu Shaobin. High-order runge-kutta discontinuous Galerkin finite element method for z-d resonator problem[J]. *Transactions of Nanjing University of Aeronautics and Astronautics*, 2008, 25(3):208-213.
- [12] Chen Eryun, Li Zhigang, Ma Dawei. Numerical simulation of unsteady-state underexpanded jet using discontinuous Galerkin finite element method [J]. *Transactions of Nanjing University of Aeronautics and Astronautics*, 2008, 25(2):89-93.
- [13] Blom C P A, Verhaar B T, van der Heijden J C, et al. A linearized Euler method based prediction of turbulence induced noise using time-averaged flow properties[R]. *AIAA 2001-1100*, 2001.
- [14] Mesbah M. *Flow noise prediction using the stochastic noise generation and radiation approach*[D]. Belgium: Katholieke Universiteit Leuven, 2006.

(Executive editor: Zhang Huangqun)